

# Influence of cycle capacity deterioration and storage capacity deterioration on Li-ion batteries used in mobile phones

Kazuhiko Takeno<sup>a,\*</sup>, Masahiro Ichimura<sup>b</sup>, Kazuo Takano<sup>b</sup>, Junichi Yamaki<sup>c</sup>

<sup>a</sup> NTT DoCoMo, 11-1, Nagatacho 2-chome, Chiyoda-ku, Tokyo 100-6150, Japan

<sup>b</sup> NTT-BTI, 3-9-11 Midori-cho, Musashino-shi, Tokyo 180-0012, Japan

<sup>c</sup> Kyushu University, 6-1, Kasuga-shi, Fukuoka 816-8580, Japan

Received 30 August 2004; received in revised form 13 October 2004; accepted 15 October 2004

Available online 2 December 2004

## Abstract

We evaluated Li-ion battery deterioration capacity characteristics that reflect the conditions under which mobile phones are actually used. Using the capacity deterioration characteristics of each cycle deterioration and storage deterioration, we show how the deterioration is influenced by the number of charge–discharge cycles and the state of charge and we show the characteristics of cycle deterioration differ from those of storage deterioration. We also show that the lifetime characteristics of a mobile phone battery is typically determined more by storage deterioration than by cycle deterioration within the pattern of the mobile phone.

© 2004 Elsevier B.V. All rights reserved.

**Keywords:** Li-ion battery; Capacity; Cycle deterioration; Storage deterioration; Impedance

## 1. Introduction

Li-ion batteries have been widely used in mobile phones recently and have contributed to remarkably improve a mobile phone's operation time because these Li-ion batteries provide a higher voltage and higher power density than either Ni–Cd or Ni–MH batteries. The Li-ion batteries used in mobile phones have LiCoO<sub>2</sub> as cathodes and graphitized carbon anodes and electrolytes of organic carbonates, and they gradually lose capacity whenever the number of charge–discharge cycles, use time, storage time, and temperature. Because a decreased battery capacity reduces both talk time and standby time, we need to know the characteristics of the deterioration of Li-ion batteries and know how to detect the end of their working lifetime in order to reduce the amount of maintenance required to keep mobile phones working properly.

The degradation of the Li-ion battery packs used in mobile phones can be quickly assessed by using impedance-measuring technology, since we have found by measuring battery capacity and the impedance at 1 kHz for various kinds of battery packs that there is a strong correlation between its capacity and this impedance [1].

There are, however, two problems that must be addressed when evaluating the characteristics of capacity deterioration. One is how to express the frequency with which the battery is used. Although mobile phone users tend to think of battery lifetime in terms of how many years (elapsed time) the battery will last, battery lifetime is typically expressed as a number of charge–discharge cycles. The lifetime of a conventional Li-ion battery is said to be about 500 cycles between the fully charged and fully discharged conditions. Figs. 1 and 2 show how the voltage–current curves and life-cycle characteristics of battery capacity change when commercial Li-ion battery packs are fully charged and fully discharged 900 times. Though the relations between the number of cycles and the capacity deterioration can be inferred from Fig. 2, the numbers of years of use cannot be estimated.

\* Corresponding author. Tel.: +81 3 5156 1321; fax: +81 3 3509 7639.

E-mail addresses: [takeno@nttdocomo.co.jp](mailto:takeno@nttdocomo.co.jp) (K. Takeno), [ichimura@ntt-bti.co.jp](mailto:ichimura@ntt-bti.co.jp) (M. Ichimura), [takano@ntt-bti.co.jp](mailto:takano@ntt-bti.co.jp) (K. Takano), [yamaki@msv.cm.kyushu-u.ac.jp](mailto:yamaki@msv.cm.kyushu-u.ac.jp) (J. Yamaki).

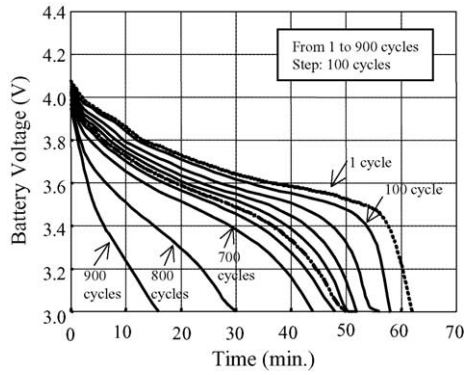


Fig. 1. Voltage curves for discharge characteristics.

The other problem is that two kinds of Li-ion battery deterioration occur at the same time: cycle deterioration and storage deterioration [2]. Cycle deterioration is due to charge–discharge cycles and depends on the number of cycles, while storage deterioration occurs when the battery is kept in a certain charge state and depends on the state of charge (SOC) and the length of the storage period. There has, however, been no research evaluating the effects of both cycle deterioration and storage deterioration on Li-ion battery lifetime. The condition under which the batteries on mobile phones operate are shown schematically in Fig. 3, where it is evident that the degrees to cycle deterioration and storage deterioration will contribute will depends on mobile phone user’s use pattern. Battery lifetime therefore cannot be predicted without taking this pattern into account.

In this paper, we present Li-ion battery capacity characteristics deterioration that reflects the use patterns of the mobile phone users. We first discuss cycle deterioration and storage deterioration characteristics (the change of capacity and impedance) that are related to the elapsed time. We then examine whether the lifetime of a mobile phone battery is influenced more by cycle deterioration or storage deterioration.

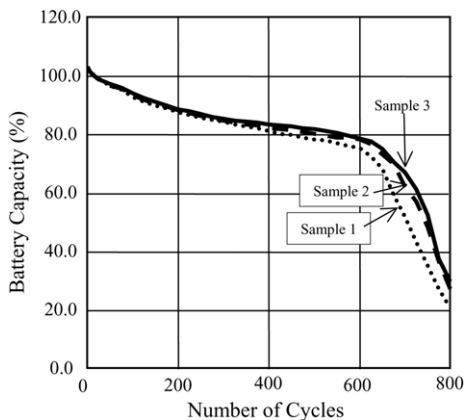


Fig. 2. Life cycle characteristics of battery capacities.

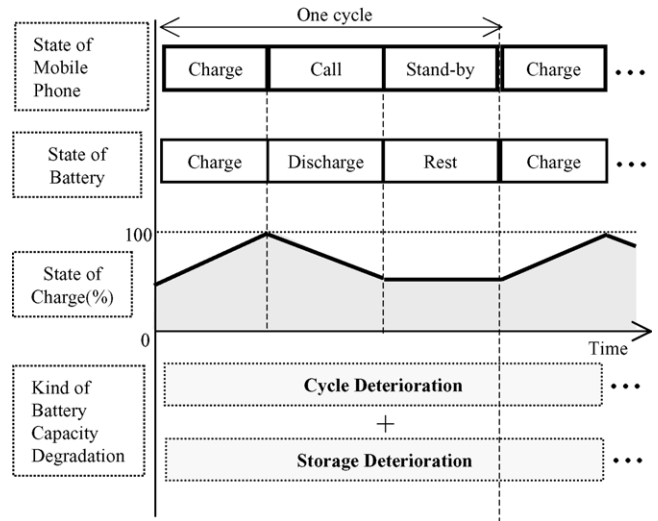


Fig. 3. Cycle and storage deterioration in Li-ion battery.

## 2. Experimental

We prepared numerous fresh and deteriorated Li-ion batteries for mobile phones. In this experiment, we used commercial Li-ion batteries (type-A) with LiCoO<sub>2</sub> as cathodes and graphitized carbon anodes. Each of the batteries was a prismatic type for a mobile phone and its capacity was 680 mA h. Deteriorated batteries were prepared by using battery charge–discharge power units and various combinations of charge–discharge cycles and storage periods. Charging method is the constant current charging (1 C mA) and constant voltage charging (4.2 V). While the deteriorated batteries were being prepared they were kept at 50 °C in an incubator to make them deteriorate rapidly.

The capacities of the deteriorated batteries were measured at room temperature (25 °C). Capacity was measured at 1 C mA discharge current to 3.0 V (the end of discharge voltage). In measuring the impedance of deteriorated batteries, we used frequency–response analysis equipment to determine the complex impedance (a system that combined the Solartron (UK) SI1287 and SI1253, which are widely used to measure the ac impedance of a battery from a range of tens of milli-Hertz to several hundreds of mega-Hertz). Using this method, we obtained a Cole–Cole plot of the Li-ion battery.

## 3. Results and discussions

### 3.1. Battery capacity and cycle deterioration

Fig. 4 shows four charge–discharge patterns for mobile phone batteries: YU-1, YU-2, YU-3, and YU-4. The initial capacity (100%) of each of the test batteries was 680 mA h. One cycle of each pattern had one full-charge (4.2 V, 1 C mA,

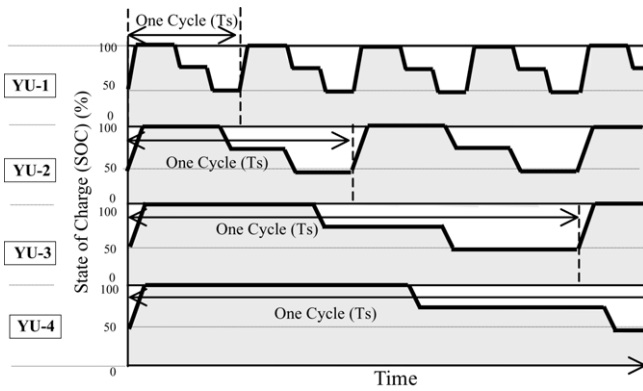


Fig. 4. Charge/discharge user cycles pattern of mobile phone's battery.

Table 1  
Experimental parameters of charge/discharge user cycles

Pattern	Ts (h)	Cycle number/day	(SOC) (%)
YU-1	3.0	8.0	75
YU-2	5.5	4.36	75
YU-3	9.5	2.53	75
YU-4	17.5	1.37	75

3 h), two 25% discharges (1 C mA, 0.25 h), and three rests periods. The parameters of the cycles shown in Fig. 4 are listed in Table 1. The average SOC ( $\langle \text{SOC} \rangle$ ) is defined as the mean charge condition of one cycle, and  $T_s$  is the period of one cycle. YU-1 is the basic pattern, and the  $T_s$  value of YU-2, YU-3 and YU-4 are longer than that of YU-1. The charge condition (4.2 V, 1 C mA, 3 h) and two discharge conditions (1 C mA, 0.25 h) are the same for all patterns in Fig. 4, and the  $\langle \text{SOC} \rangle$  of all patterns in Fig. 4 is same value (75%).

For each of the cycles shown in Fig. 4, battery capacity is plotted in Fig. 5 against elapsed time. It is obvious from this figure that the decrease rate in battery capacity is large as much as the value of the cycle time  $T_s$  is small. The battery capacity is plotted in Fig. 6 against the number of cycles. It is clear that, for the same elapsed time, the capacity decline increases in proportion to the number of cycles. Fig. 7 shows

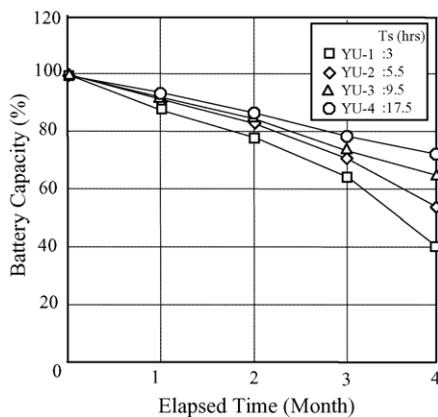


Fig. 5. Battery capacity vs. elapsed time of cycles.

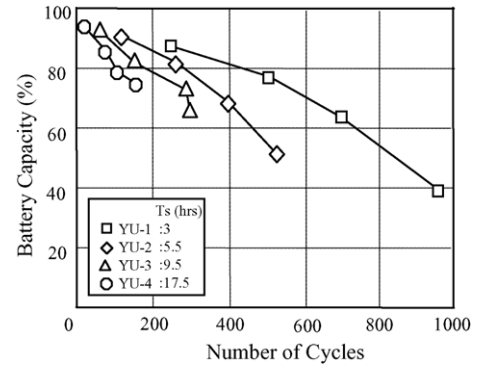


Fig. 6. Battery capacity vs. number of cycles.

the five kinds of Cole–Cole plots data for YU-2 pattern data in Fig. 5: the first for the fresh Li-ion battery and the other four for the deteriorated battery packs (1, 2, 3, and 4 months). From this figure, it is obvious that there are two changes in the curves that depend on battery deterioration. The first is the change in impedance ( $R_0$ ), in which the imaginary part is zero and the frequency is about 1 kHz.  $R_0$  increases incrementally in relation to the elapsed time (the time is related to the number of cycles). The second is the change in the two half-cycles in the Cole–Cole plots at a frequency of several hundred hertz. The diameters of the two half-cycles have increased and the centers of the two half-cycles have moved obliquely to the upper right in relation to the increments in the elapsed time.

We measured battery impedance  $R_0$  by preparing many cycle deterioration batteries. The relationship between cycle-deteriorated capacity and impedance  $R_0$  (in 100% charge and 100% discharge condition) are shown in Fig. 8. It is clear from this figure that  $R_0$  data for impedance at 1 kHz is strongly related to battery deterioration.

The impedance  $R_0$  is considered to be mainly due to the resistance between the anode and cathode. The cross sections of the anode and cathode of a Li-ion battery are shown schematically in Fig. 9, where the resistance element of  $R_0$

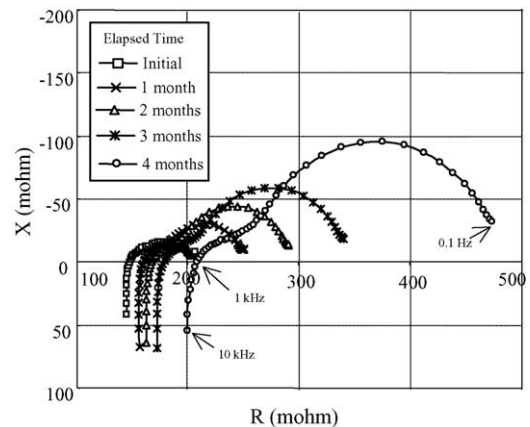


Fig. 7. Cole–Cole plots of capacity deterioration. Characteristics in user charge/discharge cycles (YU-2).

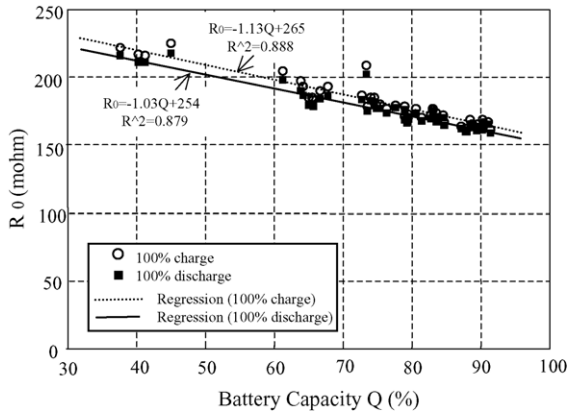


Fig. 8. Linear regressions (cycle deteriorated batteries).

comprises the resistance ( $R_{\text{electrolyte}}$ ) of the electrolyte, the resistance ( $R_{\text{SEI}}$ ) of the Solid Electrotype Interface (SEI) layer in the anode, and the contact resistance ( $R_{\text{contact}}$ ) between the active materials and current collectors. The increase in the impedance  $R_0$  is thought to be mainly due to SEI layers. It is the compound product of the Li-ion (active material) and the electrolyte growing in accordance with the charge of anode electrode and to the contact between the particles of active material (carbon) being loosened by the repeated charge–discharge cycles. The decrease in liquid electrolyte is also thought to increase  $R_0$  by decreasing the amount of conduction through the electrolyte [3,4].

3.2. Storage deterioration tests and elapsed time

Storage deterioration was evaluated considering the mobile phone’s battery storage patterns H-1, H-2, and H-3 shown in Fig. 10. These patterns have three SOC ( $\langle \text{SOC} \rangle$ ) levels: 100%, 75%, and 50%. The relations between capacity and the elapsed time and the SOC of batteries charged and discharged in these patterns are shown in Figs. 11 and 12. We

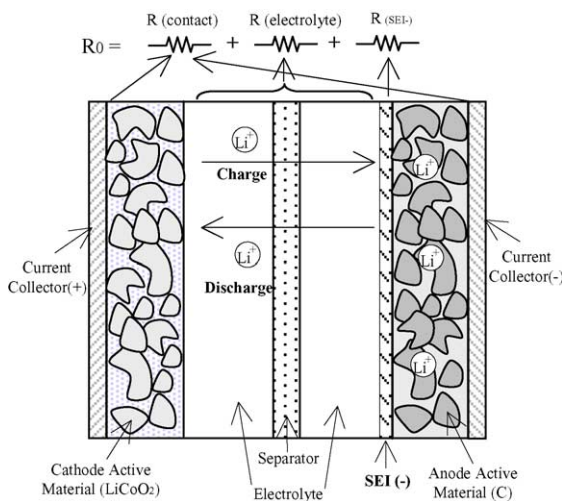


Fig. 9. Outline figure in both electrode section of Li-ion battery.

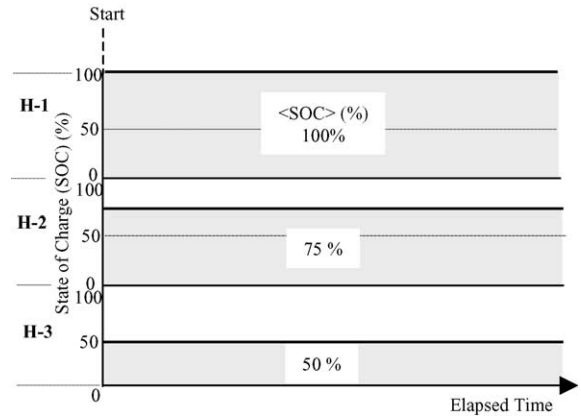


Fig. 10. Storage pattern of mobile phone’s battery.

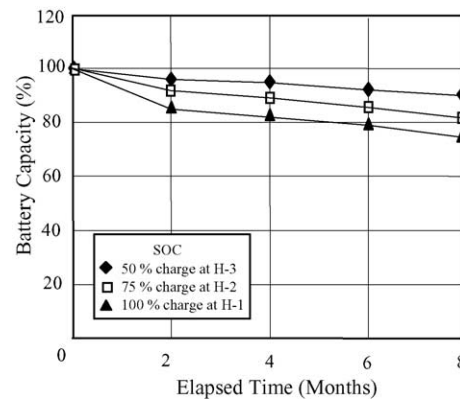


Fig. 11. Battery capacity characteristics on storage deterioration.

measured the capacities by discharging the batteries once in 2 months and recharging them to the initial state. According to these figures, it is obvious that the decrease rate in battery capacity is increase with the state of charge and that the battery deterioration is worst when its charge is kept at 100%.

Cole–Cole plots for the H-2 charge–discharge pattern are shown in Fig. 13. The first plot is for a fresh battery pack and the other four are for deteriorated battery packs (2, 4, 6, and 8 months). It is obvious that, as in Fig. 7, there are two kinds of changes that depend on battery deterioration.

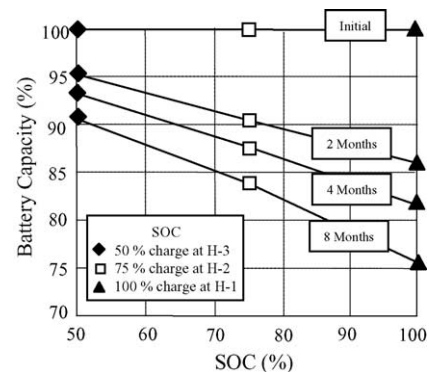


Fig. 12. Battery capacity vs. state of charge.

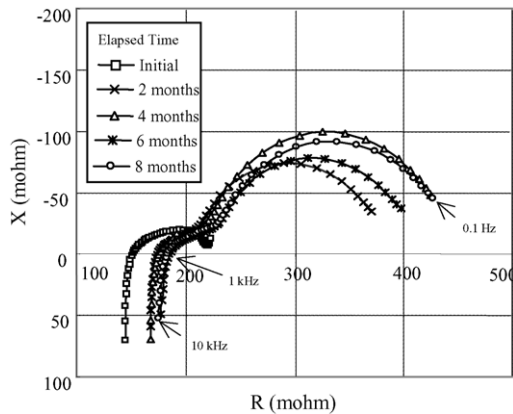


Fig. 13. Cole–Cole plot of capacity deterioration characteristics in storage deterioration at H-2 (75%).

One is the change in 1-kHz impedance ( $R_0$ ), which increases incrementally with increasing storage time. The other is that the diameters of the two half-cycles increase with the storage time.

We measured battery impedance  $R_0$  by preparing many storage deterioration batteries. The relations between battery capacity and impedance  $R_0$  is shown in Fig. 14 for batteries deteriorated in the H-2 pattern and measured in two states of charge (75% and 100%). It is obvious from this figure that, as in Fig. 8,  $R_0$  is strongly related to the degree of battery deterioration. We think that the increase of  $R_0$  is mainly due to an increased SEI(–) resistance at the anode because that is where most of the Li ions are stored.

We consider the difference between the impedance  $R_0$  characteristics of the cycle deterioration and the impedance  $R_0$  characteristics of the storage deterioration. The  $R_0$  regressions for the cycle deterioration (Fig. 8) and storage deterioration (Fig. 14) of type-A batteries are compared in Fig. 15, where it is evident that characteristics of cycle deterioration and storage deterioration are almost the same even though the rate of  $R_0$  increase is a little larger for storage deterioration. The corresponding data for 680 mA h Li-ion batteries made by another Japanese battery manufacturer (type-B

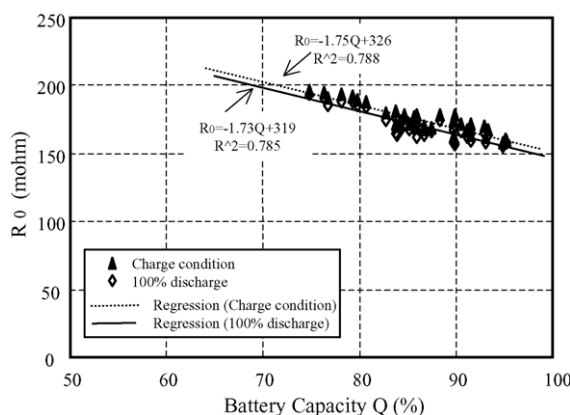


Fig. 14. Linear regressions (storage deteriorated batteries).

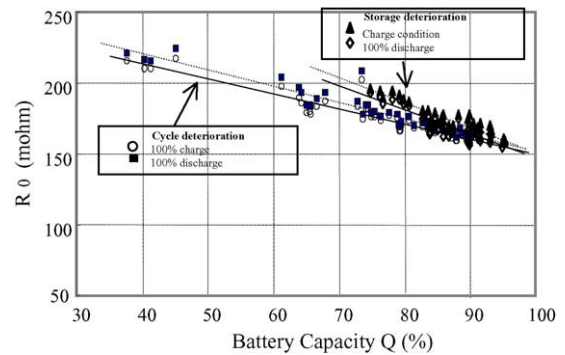


Fig. 15. Comparison of regressions between cycles and storage deterioration (type-A).

batteries) is shown in Fig. 16. This figure indicates that the impedance  $R_0$  characteristics of cycle deterioration and storage deterioration are almost the same even though the rate of  $R_0$  increase is a little lower for storage deterioration. The rates of  $R_0$  increase for cycle deterioration are almost same in Figs. 15 and 16, but the rates of  $R_0$  increase for storage deterioration differ between the two figures.

### 3.3. Battery deterioration due to both of cycle and storage deterioration

The capacity of mobile phone batteries seems to be decreased by both cycle deterioration and storage deterioration, and the degree to which each contributes to the total capacity deterioration may depend on use pattern. We therefore measured the battery capacity deterioration characteristics for both cycle deterioration and storage deterioration by using the various test patterns of mobile phone.

The test pattern we used for matrix-cycle tests is shown in Fig. 17, where the horizontal axis shows the elapsed time and vertical axis shows the SOC. During one cycle ( $T_s$ ), there is a 3-h period of charge (1 C mA and 4.2 V), a discharge (0.5 C mA) time  $T_a$ , and a rest. Here, we define  $\langle \text{SOC} \rangle$  as the mean of SOC for one cycle. According to Fig. 17, the  $\langle \text{SOC} \rangle$

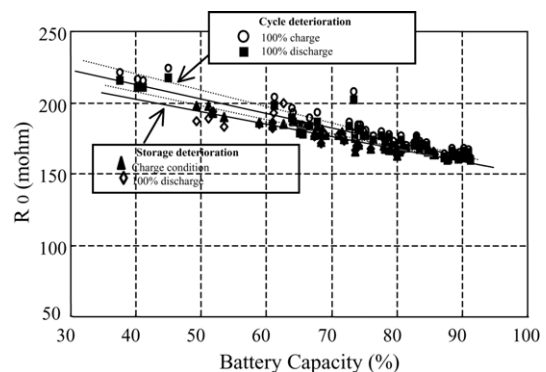


Fig. 16. Comparison of regressions between cycles and storage deterioration (type-B).



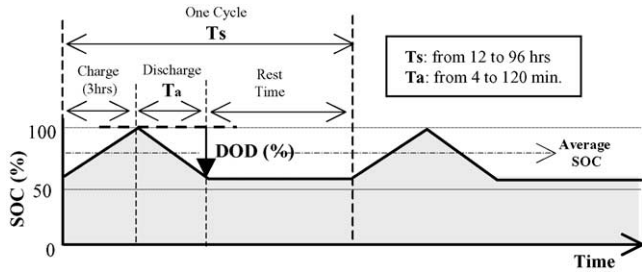


Fig. 17. Test pattern of battery matrix-cycle tests.

Table 2  
Parameters of battery deterioration tests

Ta (min)	DOD (%)	⟨SOC⟩ (%)			
		Ts = 12 h	Ts = 24 h	Ts = 48 h	Ts = 96 h
120	100	20.8	10.4	5.2	2.6
60	50	58.3	54.2	52.1	51.0
30	25	78.6	76.8	75.9	75.5
15	12.5	89.2	88.3	87.9	87.7
8	6.25	94.6	94.2	94.0	93.9
4	3.125	97.3	97.1	97.0	96.9

is shown in the following equations.

$$\langle \text{SOC} \rangle (\%) = \frac{(100 - \text{DOD} (\%))T_s + (\text{DOD} (\%)/2)(3 \text{ h} + T_a)}{100 \times T_s} \times 100 \quad (1)$$

$$\therefore \text{DOD} (\%) = 0.5 C_{\text{mA}} \times T_a \times 100 \quad (2)$$

The ⟨SOC⟩ and DOD when the parameters Ta and Ts of the test pattern is made to change are shown in Table 2. Ta is changed from 4 to 120 min, and Ts is changed from 12 to 96 h. Using these parameters (Ta, Ts), we measured the capacity of Li-ion batteries (type-A, 680 mA h) in these experiments in which we again set the temperature to 50 °C to speed deterioration.

We indicate that the relations between the battery capacity and the test pattern elapsed time Ts of 12, 24, 48, and 96 h are shown in Figs. 18–21. The discharge time Ta of the test pattern was made to change from 4 to 120 min. From these figures, it is obvious that the battery capacity decreases with the elapsed time, and the rate at which battery capacity decrease is small as much as the value of Ta (except in Fig. 18). From these results, it is understood that the average SOC influences the battery storage deterioration strongly because Ta and the average SOC are inversely proportional (Table 2). The battery capacity characteristics shown in Fig. 18 (Ts = 12 h), however, differ from those shown in Figs. 19–21. In Fig. 18 the rate at which battery capacity decrease when the Ta is 120 min is greater than that at which it decreases when Ta is 60 min.

Data of Figs. 19–21 is plotted in Fig. 22, where for Ts value of 12, 24, 48, and 96 h the capacity data measured after

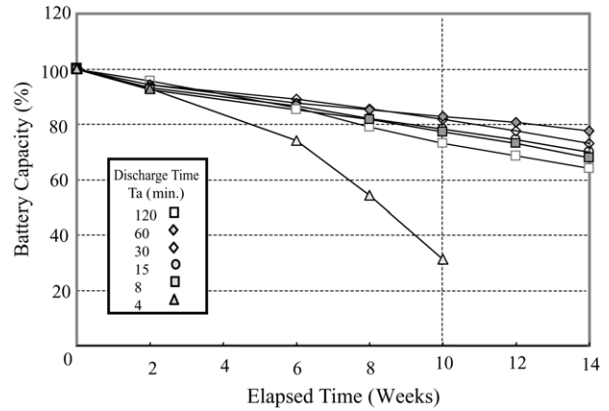


Fig. 18. Battery capacity decrease ratio vs. elapsed time with charge period (Ts = 12 h).

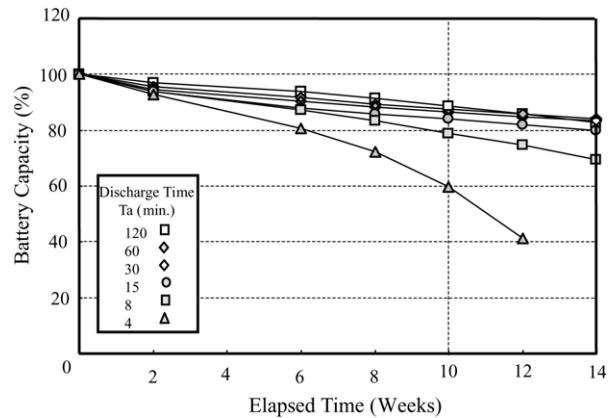


Fig. 19. Battery capacity decrease ratio vs. elapsed time with charge period (Ts = 24 h).

10 weeks elapsed is plotted against Ta. Here, it is said that the time acceleration factor becomes about five times when the temperature of the accelerating tests was 50 °C in Fig. 24. The factor estimation is based on the law of Arrhenius that the acceleration factor is two times when the temperature rises 10 °C [2]. Therefore, Fig. 22 shows the battery deterioration

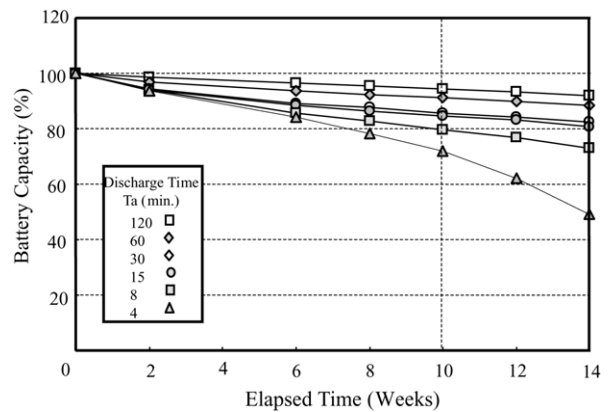


Fig. 20. Battery capacity decrease ratio vs. elapsed time with charge period (Ts = 48 h).

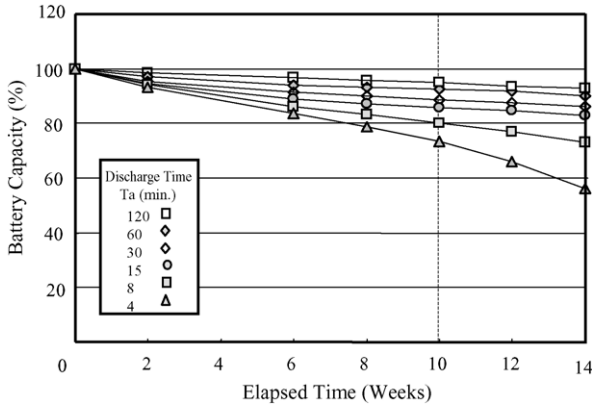


Fig. 21. Battery capacity decrease ratio vs. elapsed time with charge period ( $T_s=96$  h).

characteristics at  $25^\circ\text{C}$  (near room temperature) after about 1 year passed under the supposition of Arrhenius law.

From Fig. 22, it is obvious that the battery capacity at any  $T_a$  decreases with the decrease of  $T_s$  because the number of cycles is as much as  $T_s$  is short (from Fig. 23). It is thought that this phenomenon is battery characteristics with the influence of cycle deterioration. Furthermore, the battery capacity at almost  $T_s$  tends to decrease as  $T_a$  decreases. It is thought that this phenomenon is battery characteristics with the influence of the storage deterioration because the SOC is small as  $T_a$  is large (from Fig. 24). However, the battery capacity decrease with the increase of  $T_a$  (the range from 30 to 120 min) when  $T_s$  is 12 h in Fig. 22. We can see from the parameters listed in Table 2 and the values plotted in Fig. 25 that, in this  $T_a$  range, the value of SOC is small and the DOD is large. Therefore, the above phenomenon is thought to indicate that the increase effect of the cycle deterioration was beyond more than the decrease effect of storage deterioration. Specially, it is thought that the influence of the DOC appears when deep charge–discharge (about 100% DOD) is repeated in a short time (about 12 h).

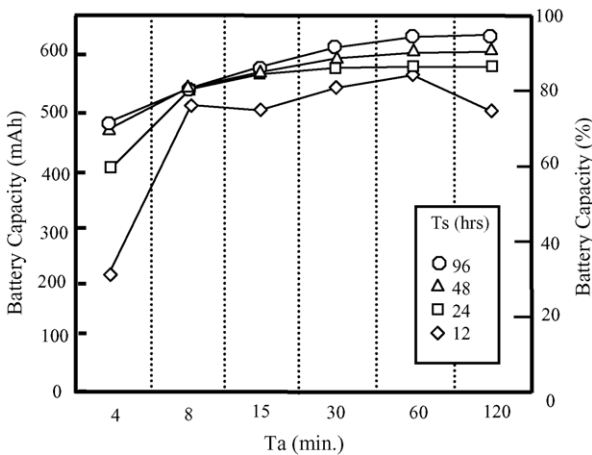


Fig. 22. Battery capacity vs. discharge time per day after 10 weeks elapsed.

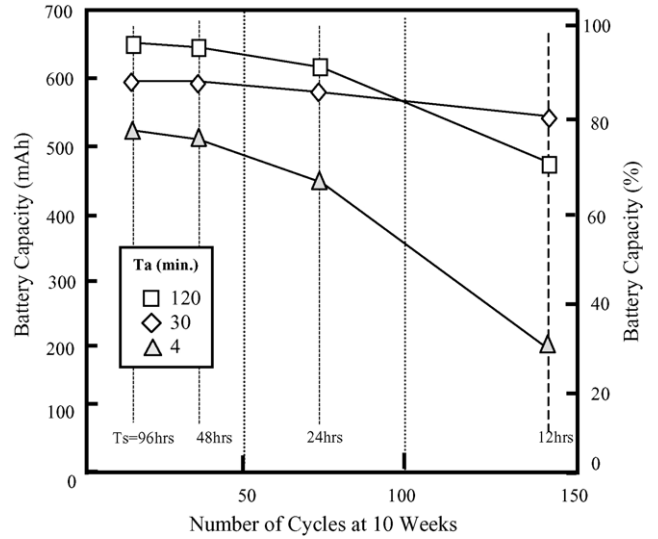


Fig. 23. Battery capacity vs. number of cycles at 10 weeks.

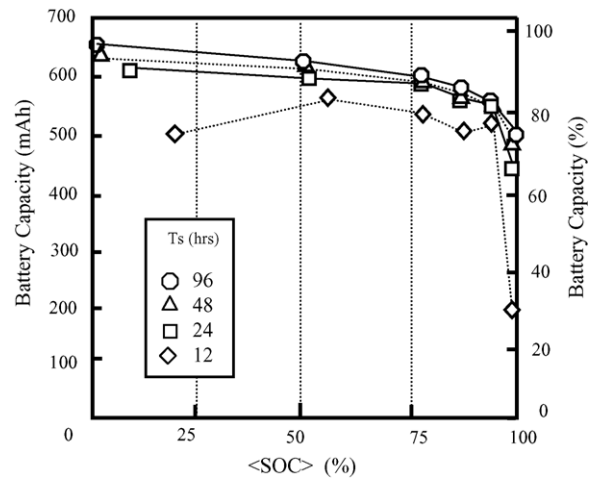


Fig. 24. Battery capacity vs. (SOC).

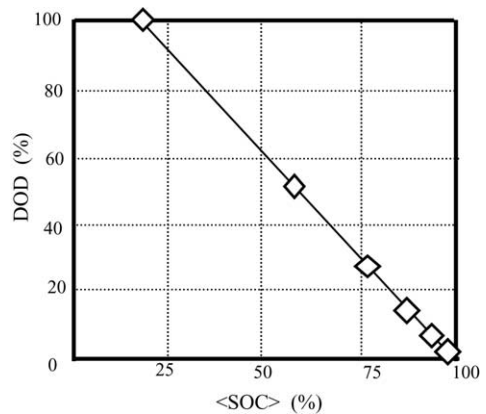


Fig. 25. Relationship between (SOC) and DOC at 12 h of  $T_s$ .

We also examined the results plotted in Figs. 22–24 from the viewpoint in battery use pattern. Here, it is considered that  $T_a$  is the same as the talk time of the mobile phone. When  $T_a$  is 4 min in Fig. 22, the battery capacity was between 31.4% and 73.3% of initial capacity. This pattern ( $T_a = 4$  min) is presumed to be that of a mobile phone user who charges the battery regularly even though he or she does not use the mobile phone much (a “light user”). When  $T_a$  is 120 min, the battery capacity was between 73.1% and 94.8% of initial capacity. This pattern ( $T_a = 120$  min) is presumed to be that of a user who charges the battery regularly and uses it for a long time (a “heavy user”). When  $T_a$  is 30 min, the battery capacity was between 82.9% and 88.5% of initial capacity. This pattern ( $T_a = 30$  min) is presumed to be that of a user who charges the battery regularly and uses the mobile phone an average amount (an “average user”). From Fig. 22, we can see that the capacity decrease rate of a heavy user ( $T_a = 120$  min) is generally small than that of a light user ( $T_a = 4$  min) though the decrease rate depends on charge period ( $T_s$ ) a little. This result means that storage deterioration is more important than cycle deterioration because DOD ( $T_a$ ) and SOC were inversely proportion when the test temperature was 50 °C.

#### 4. Conclusions

We discussed the characteristics of Li-ion battery deterioration capacity that reflect the pattern of mobile phone user’s use. From the data measured for each cycle deterioration and storage deterioration characteristic (change of capacity and impedance), which contain information about the elapsed time, we evaluated the relation between the battery parameters (the number of cycles, and the state of charge) and battery capacity deterioration. We found that the rate of capacity decline increases in proportion to the number of cycles and to the average charge. We also found that, with regard to

the battery impedance characteristics, the storage deterioration and cycle deterioration are almost the same. We further found that the lifetime of a mobile phone battery is affected more by storage deterioration than by cycle deterioration. Therefore, we guessed that the growing of SEI thickness by storage is larger than cycling.

By evaluating battery capacity deterioration data with regard to both cycle deterioration and storage deterioration, we found that the characteristics of the two kinds of deterioration reflect the pattern of a mobile phone user’s use. Finally, we found that the lifetime of a mobile phone battery is determined largely by storage deterioration because DOD and SOC were inversely proportional when the battery was tested at 50 °C.

#### Acknowledgments

We thank Mr. Mitsuo Echizenya, and Mr. Kouji Chiba of NTT DoCoMo for their kind cooperation. We also thank to Mr. Toshio Horie and Mr. Makoto Shimomura of NTT-BTI for their carrying out much of the experimental work and are also grateful for the helpful discussions they had with Dr. Katsuichi Yotsumoto of NTT-BTI.

#### References

- [1] K. Takeno, M. Ichimura, K. Takano, J. Yamaki, S. Okada, Quick testing of batteries in lithium-ion batteries packs with impedance-measuring technology, *J. Power Sources* 128 (2004) 67–75.
- [2] S.S. Choi, H.S. Lim, Factors that affect cycle-life and possible degradation mechanisms of a Li-ion cell based on  $\text{LiCoO}_2$ , *J. Power Sources* 111 (2002) 130–136.
- [3] J. Li, E. Murphy, J. Winnick, P.A. Kohl, Studies on the cycle life of commercial lithium ion batteries during rapid charge–discharge cycling, *J. Power Sources* 102 (2001) 294–301.
- [4] W.A. van Schalkwijk, B. Scrosati, *Advances in Lithium-Ion Batteries*, Kluwer Academic/Plenum Publishers, New York, 2002, pp. 393–432.